Journal of Thermal Analysis and Calorimetry
https://doi.org/10.1007/s10973-024-13096-6

A novel time-dependent analytical model for optimizing efficiency and valve timing in Ericsson engines

Panteleimon Tzouganakis[1] · Vasilios Gakos[1] · Christos Kalligeros[1] · Christos Papalexis[1] · Vasilios Spitas[1]

Received: 12 August 2023 / Accepted: 16 March 2024

Abstract

In this work, a novel analytical time-sensitive model for Ericsson engines was developed taking into account the heat transfer phenomena between the working gas and the cylinder walls in the compressor and the expander. For the calculation of the mass flow entering/exiting each cylinder, another dedicated flow model was developed to account for the pressure drop at the valves. From the energy equilibrium taking into consideration the time-dependent thermal response of the cylinder walls and the enthalpy entering/exiting each cylinder through the valves, an analytical solution of the working gas pressure and temperature can be obtained for every time step and consequently, the thermal efficiency of the engine can be calculated. A case study was performed where the thermal efficiency of an Ericsson engine was calculated for different rotational speeds and heat exchanger gas temperatures. It was observed that with higher temperatures thermal efficiency maintained a more stable behaviour with a weak dependence on rotational speed. The thermal efficiency of the engine in the performed case studies was found in the range of 10% to 14%. The valve timing of the Ericsson engine was optimized in order to achieve the highest thermal efficiency possible. The thermal efficiency of the engine could be increased up to 26% as a percentage after a thorough optimization of the valve timing. Finally, backflow phenomena accounting for thermal efficiency drop were studied. The developed model can also be applied to other types of external combustion engines such as Stirling engines.

Keywords Ericsson engine · External combustion engine · Analytical model · Valve timing · Optimization

List of symbols

Bi	Biot number
C_p	Specific heat at constant pressure (J/kg^{-1} K^{-1})
C_v	Specific heat at constant volume (J/kg^{-1} K^{-1})
D	Cylinder diameter (m)
EVC	Exhaust valve closed (deg)
EVO	Exhaust valve open (deg)
h	Coefficient of heat convection (w/m^{2}K)
IVC	Inlet valve closed (deg)
IVO	Inlet valve open (deg)
L	Cylinder wall thickness (m)
m	Mass (kg)
M	Molar mass of working fluid (kg)
n	Rotational speed of engine (rpm)
P	Pressure (bar)
Q	Heat transfer (J)
R	Universal gas constant (J K^{-1} mol^{-1})
S	Piston stroke (m)
T	Temperature (K)
U	Internal energy (J)
V	Volume (m^3)
W	Output work (J)

Greek

γ	Specific heat ratio
η_{th}	Thermal efficiency
θ	Crank angle (rad)
λ	Crank radius to rocker arm length ratio
ρ	Density (kg^{-1} m^3)

Subscripts

c	Compressor
cl	Clearance
cyl	Cylinder
d	Downstream
e	Expander
h	Heater
new	New condition
old	Old condition

✉ Panteleimon Tzouganakis
p_tzoug@hotmail.com

[1] Laboratory of Machine Design, National Technical University of Athens, 9 Iroon Polytechniou, 15780 Zografou, Greece

Published online: 17 April 2024

r Regeneration
sw Swept

Introduction

The ongoing climate change attributed to the rise of greenhouse gas levels in Earth's atmosphere [1] has led to efforts to reduce fossil fuel consumption in order to prevent global warming. Internal combustion engines have been used extensively in the industry due to the advantages they possess [2]. However, since their operation is based on fossil fuel, their replacement has been a significant goal for researchers and the industry. External combustion engines can operate with a plethora of energy sources [3–5], i.e., solar [6–8], bio-fuel [9] and waste heat [10] and therefore could be used as an alternative engine that could lead to fossil fuel reduction. The most common external combustion engines are the Stirling and Ericsson engines. The working gas in external combustion engines is usually an ideal gas that is circulated between the engine components.

Several types of Stirling engine configurations (alpha, beta and gamma) have been proposed in the literature depending on the arrangement of pistons and heat exchangers [1]. Beta-type Stirling engines are the most common ones and have been studied extensively in the literature [1]. A displacer and power piston are coupled with a rhombic drive mechanism in order to circulate the working gas between the compression and expansion space and the heat exchangers (cooler, regenerator and heater). The modelling of beta-type Stirling engines has been carried out using analytical models [11–16], CFD techniques [17] and experimental methods [18]. The governing equations of the analytical models are derived from the first thermodynamic law usually employing ideal gas formulation for each control volume of the engine (expansion and compression space and heat exchangers) [11]. For the improvement of the accuracy of the model, various loss mechanisms are included, i.e., shuttle loss [13], pressure drop in the heat exchangers and finite speed of pistons [14, 15]. Furthermore, the time-dependent thermal response of the cylinder wall and pistons has been recently investigated by the authors in order to determine the heat transfer phenomena with higher accuracy [19]. In general, one of the limitations of the analytical models is the accurate calculation of the thermal convection coefficient in each control volume of the engine at different conditions, i.e., temperature, pressure gas flow velocity. In the literature, approximations with empirical formulas of the thermal convection coefficient are typically used, which could result in an inaccurate calculation of the heat transfer [14–16, 19]. As a consequence, the thermal efficiency of the engine is in general calculated with lower accuracy (10–15% error in thermal efficiency [1]). In order to increase accuracy CFD analysis is carried out, however at a higher computational cost compared to analytical models. As a consequence, CFD models are not suitable for iterative calculations (i.e., as in optimization) and the use of analytical models may provide both adequate accuracy and fast computation. The GPU-3 engine developed by General Motors and tested by NASA has been accepted as the global benchmark for beta-type Stirling engines in the literature [18].

On the other hand, Ericsson engines are comprised of a piston-type compressor and expander. The working gas enters the compressor at a given pressure (in most cases at atmospheric pressure and ambient temperature) where it is compressed and sent to the heat exchanger. The working gas is heated therein and then enters the expander, where the output mechanical power is generated. Finally, a regenerator is usually employed in order to increase the efficiency of the engine [20]. The work produced and the thermal efficiency of the engine depending on cylinder geometry (diameter and stroke), the geometry of the crank-slider mechanism, the temperature of the heat exchanger, the rotational speed of the engine and the timing of the valves in the compressor and expander. A CFD analysis could describe the phenomena of an Ericsson engine with high accuracy, however, the computational cost would be high due to the required precision in the modelling of the valves in the two cylinders and the heat exchanger. Several numerical and analytical models on the operation of the Ericsson engine have been proposed in the literature [20–22]. However, these models assume ideal Ericsson or Joule cycles in the compressor and expander which is not the case under real operating conditions mainly due to heat losses from the working gas to the cylinder walls. As a consequence, the thermal efficiency of the engine is in general overestimated and optimal design may not be achieved. Furthermore, valve timing in the compressor and the expander is an important design parameter in Ericsson engines [23]. An analytical full model of an Ericsson engine taking into consideration the inherent geometry, valve timing, temperature of the heat exchanger and time-dependent heat transfer between the working gas and the cylinder walls would be beneficial in improving the optimization of Ericson engine performance.

In the present research, an analytical model of Ericsson engines is developed taking into account the time-dependent thermal response of the cylinder wall in the compressor and expander. The operation of the valves will be modelled in order to calculate the mass flow of the working gas entering/exiting each cylinder at each time step of the operation. The pressure and temperature of the working gas at each cylinder will be obtained taking into consideration the first thermodynamic law for an open system, the ideal gas law and the motion equation of the piston. Therefore, an analytical expression for the working gas pressure can be derived for each time step of the operation.

As a consequence, the PV diagrams can be obtained for the steady-state operation (convergence of the cylinder wall temperature in the compressor and expander) and the thermal efficiency of the engine can be determined. A case study was performed for different temperatures in the heat exchanger and different rotational speeds of the engine. It was observed that with higher temperatures in the heat exchanger, the thermal efficiency of the engine had a more stable behaviour. Furthermore, a sensitivity analysis was performed on the valve opening timing in the compressor and expander. It was illustrated that valve timing constitutes one of the most important parameters of the design of Ericsson engines. The thermal efficiency of the engine could be significantly improved after the optimization of the valve timing. Finally, backflow phenomena have been observed due to valve operation that would result in lower thermal efficiency of the engine.

To our knowledge, there is no transient thermal modelling of Ericsson engines that takes into consideration the heat transfer phenomena between the working gas and the cylinder walls. Therefore, the developed model could be a valuable design tool for the Ericsson engines due to the accuracy of the model through the detailed analysis of the heat transfer phenomena. The computational cost of the model is low since the pressure and temperature of the working gas can be calculated analytically at each time step. Therefore, with the proposed model the optimization of the dimensions of the cylinder and the valve timing could be achieved with accuracy and low computational cost. The developed model could also be implemented in other external combustion engines, i.e., Stirling engines since the energy equilibriums at each control volume are similar to cylinder modelling in the Ericsson engines.

Modelling of Ericsson engine

In Fig. 1, a typical Ericsson engine is presented. The working gas enters the compressor at a given pressure where it is compressed to a certain pressure and sent to the heat exchanger. The working gas is heated in the heat exchanger and then enters the expander, where the mechanical work is produced. Finally, a regenerator in the exhaust of the expander is usually used in order to increase the efficiency of the engine. For the analysis of the operation of the engine an analytical model for the valve operation, the heat transfer phenomena and the analysis of the thermodynamic phenomena is required.

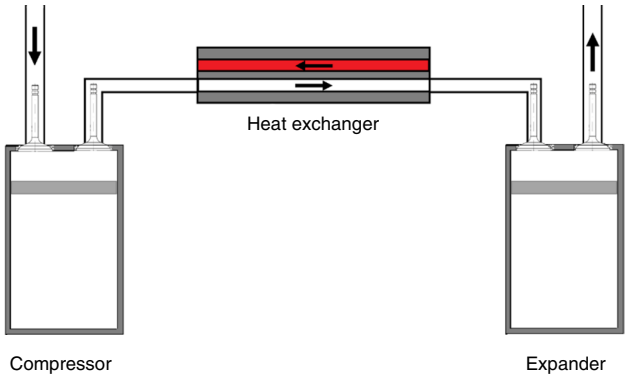

Fig. 1 Ericsson engine configuration

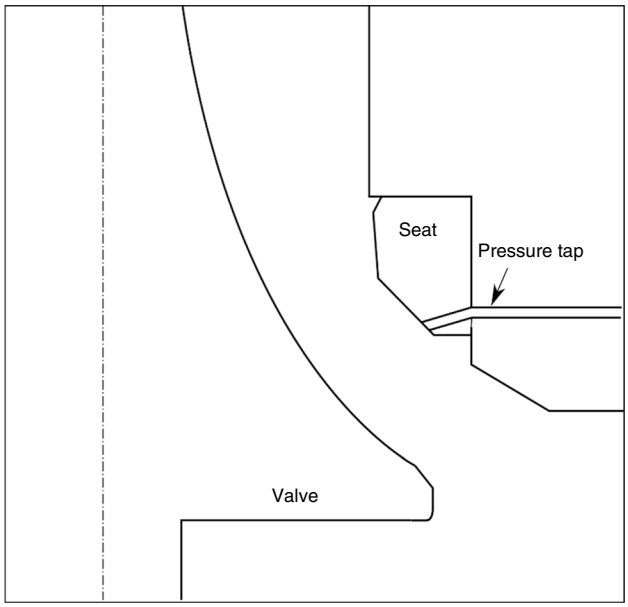

Fig. 2 Typical cylinder valve geometry

Gas flow through valves

The circulation of the working medium in the compressor and the expander is performed with valves, that open and close at specific crank angles during the cycle. A typical valve is shown in Fig. 2. The mass flow rate entering/exiting the valve is [24]:

$$\dot{m} = C_{\mathrm{d}} A_{\mathrm{ref}} \frac{p_{\mathrm{u}}}{\sqrt{R T_{\mathrm{u}}}} \left(\frac{p_{\mathrm{d}}}{p_{\mathrm{u}}}\right)^{\frac{1}{\gamma}} \left\{ \frac{2\gamma}{\gamma - 1} \left[1 - \left(\frac{p_{\mathrm{d}}}{p_{\mathrm{u}}}\right)^{\frac{\gamma-1}{\gamma}} \right] \right\}^{\frac{1}{2}} \quad (1)$$

where C_{d} is the discharge coefficient through the constriction which is considered equal to 0.7 [24], A_{ref} is the minimum cross-sectional area of flow constriction, $p_{\mathrm{u}}, T_{\mathrm{u}}$ are the

pressure and temperature upstream of the valve and p_d is the pressure downstream of the valve.

The opening l of the valve can be calculated from Eq. (2) [24]:

$$l(\theta) = \frac{L_{\max}}{2}\left[1 - \cos\left(2\pi\frac{(\theta - \theta_0)}{\delta\theta}\right)\right] \tag{2}$$

where $L_{\max}$ is the maximum valve lift, θ_0 is the valve opening angle and $\delta\theta$ is the window when the valve remains open.

The cross-sectional area of the gap can be calculated from Fig. 3 through Eq. (3)

$$A_{\text{ref}} = \pi(r_1 + r_2)\sqrt{(r_1 - r_2)^2 + l^2} \tag{3}$$

The minimum cross-sectional area for each crank angle can be calculated numerically from Eq. (2), (3) [24].

Heat transfer in cylinder walls

The time-dependent thermal response of the cylinder wall can be obtained from the heat transfer between the cylinder wall and the working gas in the compressor and the expander. The Biot (Bi) number is:

$$\text{Bi} = \frac{Lh}{k} \tag{4}$$

where L is the thickness of the wall, h is the convection coefficient of the gas and k is the thermal conductivity of the metal. The Biot number is small (< 0.1) since the wall thickness is small and the thermal conductivity is high. Therefore, the cylinder wall can be modelled as a lumped system where the temperature is steady throughout the thickness of the wall as follows:

$$h_{\text{cyl}}A\left(T_{\text{cyl}} - T_{\text{wall}}\right) + h_{\text{air}}A\left(T_{\text{air}} - T_{\text{wall}}\right) = mC_{\text{p}}\frac{\mathrm{d}T_{\text{wall}}}{\mathrm{d}t} \tag{5}$$

where h_{cyl} and T_{cyl} are the convection coefficient and the temperature of the working gas in the cylinder, h_{air} and T_{air} are the convection coefficient and the temperature of the air outside of the cylinder, A is the surface area of the cylinder, $m, C_{\text{p}}, T_{\text{wall}}$ are the mass, the heat capacity and the temperature of the cylinder wall. As a result, the new temperature of the cylinder wall in the next time step is:

$$T_{\text{wall,new}} = \left(T_{\text{wall,old}} - \frac{h_{\text{cyl}}T_{\text{cyl}} + h_{\text{air}}T_{\text{air}}}{h_{\text{cyl}} + h_{\text{air}}}\right) e^{-\frac{h_{\text{cyl}}+h_{\text{air}}}{\rho C_{\text{p}}L}\Delta t} + \frac{h_{\text{cyl}}T_{\text{cyl}} + h_{\text{air}}T_{\text{air}}}{h_{\text{cyl}} + h_{\text{air}}} \tag{6}$$

where $T_{\text{wall,old}}$ and $T_{\text{wall,new}}$ is the cylinder wall temperature of the previous and next time step, respectively, ρ is the density of the cylinder material and Δt is the timestep of the model.

The convection coefficient of the working fluid in the cylinder can be calculated from the Woschni formula [25]:

$$h_{\text{cyl}} = 129.8D^{-0.2}P^{0.8}T^{-0.55}W^{0.8} \tag{7}$$

where D is the diameter of the piston in m, P is the pressure for crank angle θ in bars and T is the temperature for crank angle θ in [K]. The parameter W can be defined as [25]:

$$W = c_1\frac{2Sn}{60} \tag{8}$$

where $c_1 = 2.28$ for compression and $c_1 = 6.18$ for gas exchange in the cylinder and n is the rotational speed of the engine in [rpm]. The convection coefficient as calculated from Eq. (7) is typically used in engine cylinders [19, 25], to account for the cylinder geometry and the presence of valves.

Cylinder thermodynamic cycles

The volume of the cylinder as a function of the crank angle θ can be obtained from the crankshaft equation of motion:

$$V(\theta) = \frac{V_{\text{sw}}}{2}\left(1 + \lambda - \cos\theta - \sqrt{\lambda^2 - \sin^2\theta}\right) + V_{\text{cl}} \tag{9}$$

where V_{sw} is the swept volume and V_{cl} is the clearance volume of the piston, $\lambda = r/l$ with r the radius of the crank and l is the length of the rocker arm.

The rate of change of the cylinder volume as a function of the crank angle θ is(9):

$$c(\theta) = \frac{\mathrm{dV}(\theta)}{\mathrm{d}\theta} = \frac{V_{\text{sw}}}{2}\left(\sin\theta + \frac{\sin\theta\cos\theta}{\sqrt{\lambda^2 - \sin^2\theta}}\right) \tag{10}$$

The First Law of Thermodynamics is used in order to obtain the energy equilibrium in each cylinder:

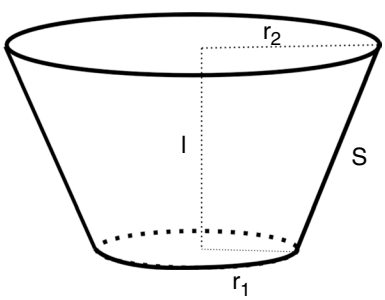

Fig. 3 Valve's cross-sectional area

$$\frac{\mathrm{d}U(\theta)}{\mathrm{d}\theta} = \frac{\mathrm{d}Q(\theta)}{\mathrm{d}\theta} - \frac{\mathrm{d}W(\theta)}{\mathrm{d}\theta} + \left(\frac{\mathrm{d}m_{\mathrm{in}}}{\mathrm{d}\theta}h_{\mathrm{in}} - \frac{\mathrm{d}m_{\mathrm{out}}}{\mathrm{d}\theta}h_{\mathrm{out}}\right) \quad (11)$$

where $h_{\mathrm{in}} = C_{\mathrm{p}}\left(T_{\mathrm{in}}\right)T_{\mathrm{in}}$ and $h_{\mathrm{out}} = C_{\mathrm{p}}\left(T_{\mathrm{out}}\right)T_{\mathrm{out}}$ are the enthalpies entering/exiting the cylinder, respectively.

The terms of Eq. 11 can be obtained as follows:

$$\frac{\mathrm{d}U(\theta)}{\mathrm{d}\theta} = \frac{30C_{v}(T(\theta))}{\pi n}[\dot{m}(\theta)T(\theta) + m(\theta)\dot{T}(\theta)] \quad (12)$$

$$\frac{\mathrm{d}W(\theta)}{\mathrm{d}\theta} = P(\theta)\frac{\mathrm{d}V(\theta)}{\mathrm{d}\theta} = P(\theta)c(\theta) \quad (13)$$

$$\frac{\mathrm{d}Q(\theta)}{\mathrm{d}\theta} = \frac{120h_{\mathrm{cyl}}V(\theta)}{\pi Dn}[T_{\mathrm{wall}}(\theta) - T(\theta)] \quad (14)$$

Finally, the ideal gas law is considered due to the assumption of ideal working gas:

$$P(\theta)V(\theta) = \frac{m(\theta)}{M}RT(\theta) \quad (15)$$

As a consequence, the following equation can be obtained:

$$\dot{T}(\theta) + \mathrm{A}(\theta)\mathrm{T}(\theta) = \mathrm{B}(\theta) \quad (16)$$

where:

$$\mathrm{A}(\theta) = \frac{\dot{m}(\theta)}{m(\theta)} + \frac{4h_{\mathrm{cyl}}V(\theta)}{C_{\mathrm{v}}(T(\theta))Dm(\theta)} + \frac{\pi nRc(\theta)}{30\mathrm{M}C_{\mathrm{v}}(T(\theta))V(\theta)} + \frac{\gamma\dot{m}_{\mathrm{out}}(\theta)}{m(\theta)} \quad (17)$$

$$B(\theta) = \frac{4h_{\mathrm{cyl}}V(\theta)T_{\mathrm{wall}}(\theta)}{C_{\mathrm{v}}(T(\theta))Dm(\theta)} + \frac{\dot{m}_{\mathrm{in}}(\theta)Cp\left(T_{\mathrm{in}}\right)T_{\mathrm{in}}}{C_{\mathrm{v}}(T(\theta))m(\theta)} \quad (18)$$

where T_{in} is the temperature of the gas that enters each cylinder and γ is the specific heat ratio.

As a consequence, from Eq. (11)-(18) the working gas temperature in each cylinder can be determined for the following time step from the analytical solution:

$$T_{\mathrm{new}} = \left(T_{\mathrm{old}} - \frac{B(\theta)}{\mathrm{A}(\Theta)}\right)e^{-A(\theta)\Delta t} + \frac{B(\theta)}{\mathrm{A}(\Theta)} \quad (19)$$

where T_{old} and T_{new} is the temperature of the working gas in the previous and the following time step respectively. Therefore, the temperature and pressure of the working gas at the compressor and expander can be determined until the steady-state operation of the engine is achieved (convergence of the cylinder wall temperature).

The work in the compressor and expander can be calculated numerically from the PV diagrams in the steady-state operation:

$$W_{\mathrm{c}} = \int_{\theta=0^{\circ}}^{\theta=360^{\circ}} P_{\mathrm{c}}(\theta)\mathrm{d}V_{\mathrm{c}}(\theta)\mathrm{d}\theta \quad (20)$$

$$W_{\mathrm{e}} = \int_{\theta=0^{\circ}}^{\theta=360^{\circ}} P_{\mathrm{e}}(\theta)\mathrm{d}V_{\mathrm{e}}(\theta)\mathrm{d}\theta \quad (21)$$

The required heat in the heat exchanger can be calculated from the temperature difference between the working gas in the heat exchanger and the temperature of the working gas in the compressor during the operation of the exhaust valve. Therefore:

$$Q_{\mathrm{h}} = \int_{\theta=\mathrm{EVO_c}}^{\theta=\mathrm{EVC_c}} \dot{m}_{\mathrm{c}}(\theta)\Delta tC_{\mathrm{p}}(T_{\mathrm{h}})(T_{\mathrm{h}} - T_{\mathrm{c}}(\theta))\mathrm{d}\theta \quad (22)$$

Furthermore, for the optimal thermal efficiency of the engine, regeneration in the expander exhaust can be used. The acquired energy assuming an ideal regenerator can be calculated as follows:

$$Q_{\mathrm{r}} = \int_{\theta=\mathrm{EVO_e}}^{\theta=\mathrm{EVC_e}} \dot{m}_{\mathrm{e}}(\theta)\Delta tC_{\mathrm{p}}(T_{\mathrm{e}}(\theta))(T_{\mathrm{e}}(\theta) - T_{\mathrm{air}})\mathrm{d}\theta \quad (23)$$

The acquired energy from the regenerator is used in the compressor. The thermal efficiency of the engine can be calculated from:

$$n_{\mathrm{th}} = \frac{W_{\mathrm{e}} - W_{\mathrm{c}}}{Q_{\mathrm{h}}} \quad (24)$$

Followed methodology

A case study is performed according to the geometrical characteristics and working conditions presented in Table 1. The temperature of the heat exchanger and the rotational speed of the engine are assumed to be constant throughout the operation of the engine.

The dimensions and timing of the valves for the compressor and expander are presented in Table 2.

Table 1 General parameters

Working fluid	Air
S	90 mm
D	30 mm
compression ratio	4
λ	5
n	1500 rpm
p_{u}	1 bar
T_{h}	1000 K
T_{u}	295 K

Table 2 Valve operational parameters

	Compressor	Expander
Max inlet lift /mm	0.1	0.5
Max exhaust lift /mm	0.2	0.5
IVO /deg	65	0
IVC /deg	180	120
EVO /deg	310	180
EVC /deg	360	330

The transient response of the Ericsson engine was obtained with an algorithm developed in MATLAB without the use of any iterative methods since the equations that describe the operation of the system are analytical. An angle step of 0.1 degrees was deemed adequate as shown in other similar studies in external combustion engines [14–16]. During transient operation, the thermal efficiency changes with respect to time especially in the first complete cycles of operation. The thermal efficiency is stabilized after approximately 500 complete cycles of operation due to the stabilization of the working gas flow through the valves.

Results and discussion

The PV diagrams of the compressor and expander during the steady-state operation are presented in Fig. 4. It can be observed that in the compressor, the pressure exceeds the pressure in the heater and as a consequence, the work required is increased and the thermal efficiency of the engine is decreased. Furthermore, the pressure in the expander is lower than the pressure of the working gas in the heater and therefore, the produced work is lower which leads to a lower thermal efficiency of the engine. Both phenomena can be attributed to the valve timing in the compressor and expander. Even though, valve timing has been optimised in order to achieve maximum thermal efficiency, it is evident that that valve timing constitutes a significant and very difficult parameter to optimize due to the transient heat transfer phenomena. It should be mentioned that the wavy profile of the PV diagram of the expander is attributed to the valve operation and not to the selected time step of the model.

For the performed case study, the work in the compressor is $W_c = 3.83$J, the work in the expander is $W_e = 6.24$J the required heat in the heat exchanger is $Q_h = 20.74$J. As a result, the thermal efficiency of the engine is 11.60%.

In Fig. 5, the working gas mass in the compressor is presented. It can be observed that during the opening of the exhaust valve of the compressor, backflow phenomena are present (Detail A). This is also evident from the PV diagram of the compressor since the pressure of the working gas in the compressor is lower than the pressure of the working gas in the heat exchanger when the exhaust valve opens. As a result, the mass flow enters the compressor from the heat exchanger increasing the pressure and the required work in the compressor and thus reducing the thermal efficiency of the engine.

In Fig. 6, the working gas temperature in the compressor is shown during the steady-state operation. The working gas temperature is decreased when the crank angle is between [0, IVO] since the pressure of the working gas is decreased as shown in Fig. 4. The temperature is decreased from 470 to 240K. When the crank angle is between [IVC, EVO] the temperature is increased since the working gas is compressed. The highest temperature is 515K and is observed during the EVO angle.

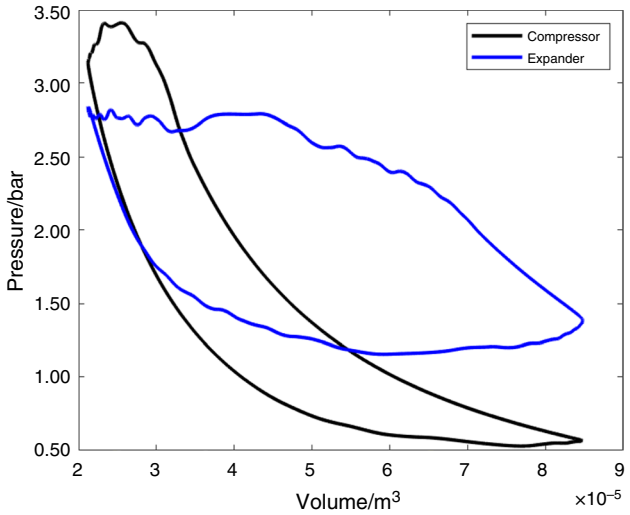

Fig. 4 PV diagrams during steady-state operation in the compressor and expander

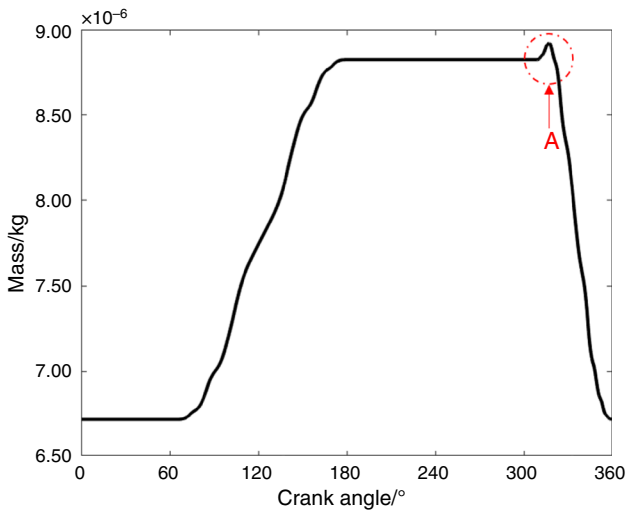

Fig. 5 PV Working gas mass in the compressor during steady-state operation

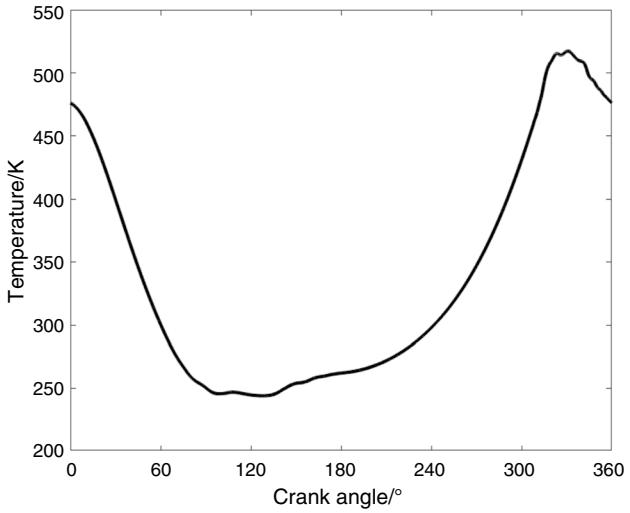

Fig. 6 PV Working gas temperature in the compressor during steady-state operation

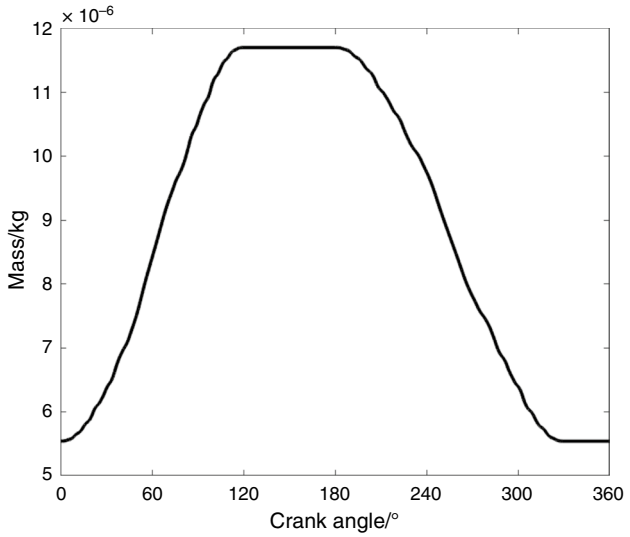

Fig. 7 PV Working gas mass in the expander during steady-state operation

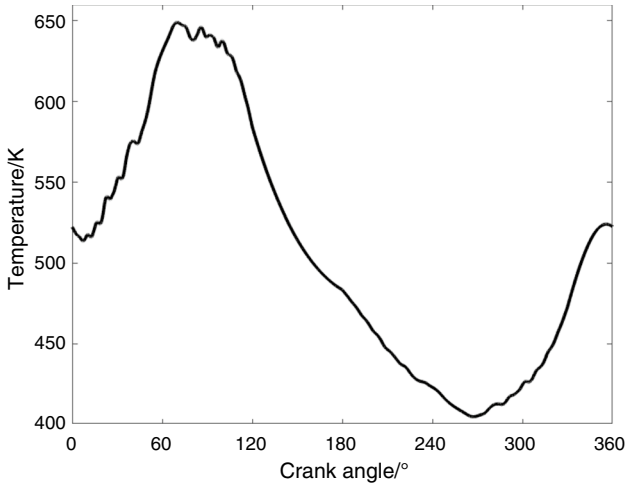

Fig. 8 PV Working gas temperature in the expander during steady-state operation

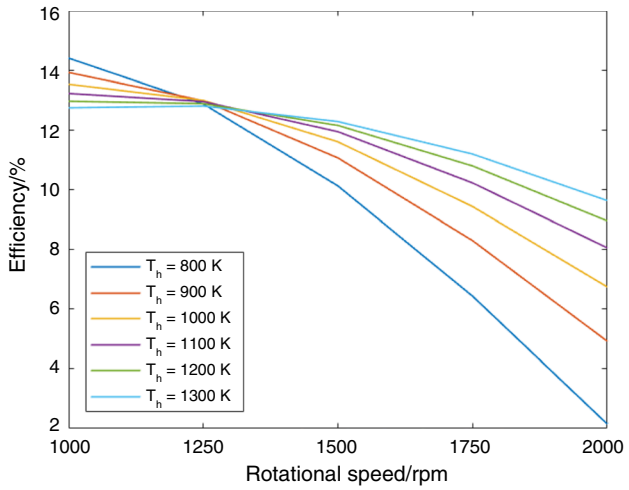

Fig. 9 Thermal efficiency for different heat exchanger temperatures and rotational speeds

In Fig. 7, the mass of the working in the expander during steady-state operation is presented. The mass of the working gas is increased when the crank angle is between [0, IVC] since gas from the heater enters the expander. When the crank angle is between [EVO, EVC] the mass of the working gas is decreased since the working gas exits the expander and enters the regenerator. No backflow phenomena are observed in the expander during the inlet and exhaust valve opening.

In Fig. 8, the working gas temperature in the expander during steady-state operation is shown. The working gas temperature is increased from 520 to 650K when the crank angle is between [0, IVC] since gas from the heater enters the expander. When the crank angle is between [IVC, EVO] the temperature is decreased since work is produced in the expander and as a consequence, the pressure is decreased during the process. The lowest temperature in the expander is 405K.

A case study was also performed for different working gas temperatures in the heat exchanger and different rotational speeds of the engine. The thermal efficiency was calculated for each case and the results are presented in Fig. 9. It can be observed that the efficiency of the engine decreases as the rotational speed of the engine increases. Furthermore, it is shown that with higher working gas temperatures in the heat exchanger, the thermal efficiency of the engine is more stable in a wider range of rotational speeds.

For example, when the heat exchanger temperature is 1300 K the efficiency of the engine is between 10 and 12.5%. On the other hand, a significant difference in the thermal efficiency of the engine at different rotational speeds can be observed in lower heat exchanger temperatures. For instance, when the heat exchanger temperature is at 800 K the efficiency of the engine is between 2 and 14%.

Finally, the effect of the valve timing in the compressor and expander was investigated. The optimal valve opening in the compressor can be approximated with the following process. The inlet valve opening time can be obtained as the angle of rotation when the working gas pressure is equal to the ambient pressure in order to reduce backflow phenomena. Similarly, the exhaust valve opening time can be obtained as the angle of rotation when the working gas pressure is equal to the pressure in the heat exchanger. However, due to time-dependent phenomena, backflow could be observed as shown in Fig. 5 for the case of the exhaust valve which would reduce the thermal efficiency of the engine in the steady-state operation. With the proposed process, the optimal valve opening time for the compressor can be approximated adequately. However, for the case of the expander, a similar process cannot be derived since the optimal pressure of working gas during the closing of the inlet and exhaust valves is unknown. As a consequence, the inlet and exhaust valve closing in the expander should be optimized in order to obtain maximum thermal efficiency. In Table 3, the efficiency of the engine for different values of IVC_e and EVC_e is presented.

The valve timing constitutes a critical parameter for the thermal efficiency of the engine and small changes could yield significant differences in the thermal efficiency of the engine. For instance, the thermal efficiency of the engine at $IVC_e = 130°$ and $EVC_e = 320°$ is 9.21%, while at $IVC_e = 120°$ and $EVC_e = 330°$ is 11.60% and as a consequence, the thermal efficiency is increased by 26% as a percentage. Therefore, the optimization of the valve timing is necessary for Ericsson engines. With the developed model an accurate and computationally low procedure is proposed in order to determine the optimal valve timing taking into consideration the time-dependent thermal phenomena during the operation of the engine.

Table 3 Efficiency (%) for different values of IVC_e and EVC_e

EVCe/deg / IVCe/deg	320	325	330	335	340
110	9.58	10.62	11.49	10.98	10.78
115	9.94	10.89	11.53	11.25	11.02
120	9.96	10.85	11.60	11.43	11.24
125	9.69	10.54	11.27	10.81	11.35
130	9.21	10.02	10.73	10.62	10.37

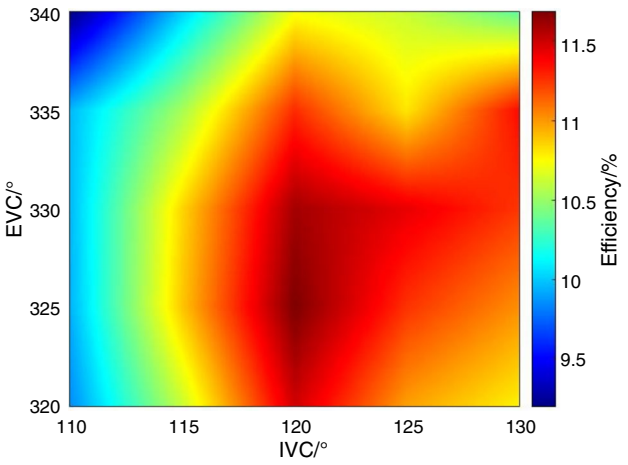

Fig. 10 Heat map of thermal efficiency for different inlet and exhaust valve closing in the expander

In Fig. 10, a heat map of the thermal efficiency of the engine is presented for different inlet and exhaust valve closing in the expander according to results presented in Table 3.

Conclusions

In the present research, a novel analytical model for the calculation of the thermal efficiency in Ericsson engines was developed. The time-dependent heat transfer phenomena between the working gas and the cylinder wall in the compressor and expander were taken into account, while the mass flow entering/exiting the valves in the compressor and expander has been modelled analytically. As a result, from the energy equilibriums at each cylinder, the ideal gas law and the motion equation of the pistons an analytical calculation of the pressure and temperature of the working gas can be derived at each time step. Therefore, the PV diagrams of the compressor and expander and the thermal efficiency of the engine for the steady-state operation (convergence of cylinder wall temperature) can be obtained. From the performed case studies, the following observations were made:

- The thermal efficiency of the engine had a more stable behaviour for a wider range of rotational speeds when the heat exchanger temperature was higher, with an efficiency between 10 and 14%.
- The critical contribution of the valve timing in the compressor and expander to the thermal efficiency of the engine was shown. It was observed that the thermal efficiency of the engine could be increased up to 26% (as a percentage) after a valve timing optimization.
- Backflow phenomena were observed during valve opening in the compressor that deteriorate the thermal efficiency of the engine.

The developed model could be a valuable design tool for researchers and the industry due to the accuracy of the model (inclusion of time-dependent heat and mass transfer phenomena) and low computational cost (analytical solution at each time step). The proposed method could also be used for other external combustion engines, i.e., Stirling engines. In future work, a more generalized optimization utilizing the developed analytical model could be an interesting research topic. A significant number of geometrical parameters in the cylinder-crankshaft mechanism and in the valves are present. Therefore, a thorough optimization could result in higher thermal efficiencies and could lead to the wider industrial application of the Ericsson engine. Furthermore, a more detailed analysis on backflow phenomena that deteriorate the efficiency of the engine could be performed.

Funding Open access funding provided by HEAL-Link Greece.

References

1. Ahmed F, Huang H, Ahmed S, Wang X. A comprehensive review on modeling and performance optimization of Stirling engine. Int J Energy Res. 2020;44(8):6098–127.
2. Ritchie H, and Roser M, "CO_2 and Greenhouse Gas Emissions," *Our World Data*, May 2020, Accessed 18 Mar 2022.
3. Campos M, Vargas JVC, Ordonez J. Thermodynamic optimization of a Stirling engine. Energy. 2012;44:902–10. https://doi.org/10.1016/j.energy.2012.04.060.
4. Costa SC, Barrutia H, Esnaola JA, Tutar M. Numerical study of the pressure drop phenomena in wound woven wire matrix of a Stirling regenerator. Energy Convers Manag. 2013;67:57–65. https://doi.org/10.1016/j.enconman.2012.10.014.
5. Sánchez D, Chacartegui R, Torres M, Sánchez T. Stirling based fuel cell hybrid systems: an alternative for molten carbonate fuel cells. J Power Sour. 2009;192(1):84–93. https://doi.org/10.1016/j.jpowsour.2008.12.061.
6. Makhkamov KK, Ingham DB. Analysis of the working process and mechanical losses in a Stirling engine for a solar power unit. J Sol Energy Eng. 1999;121(2):121–7. https://doi.org/10.1115/1.2888149.
7. Barreto G, Canhoto P. Modelling of a Stirling engine with parabolic dish for thermal to electric conversion of solar energy. Energy Convers Manag. 2017;132:119–35. https://doi.org/10.1016/j.enconman.2016.11.011.
8. Bellos E. Progress in the design and the applications of linear Fresnel reflectors—a critical review. Therm Sci Eng Prog. 2019;10:112–37. https://doi.org/10.1016/j.tsep.2019.01.014.
9. Mahkamov K. Design improvements to a biomass stirling engine using mathematical analysis and 3D CFD modeling. J Energy Resour Technol. 2005;128(3):203–15. https://doi.org/10.1115/1.2213273.
10. Wang K, Sanders SR, Dubey S, Choo FH, Duan F. Stirling cycle engines for recovering low and moderate temperature heat: a review. Renew Sustain Energy Rev. 2016;62:89–108. https://doi.org/10.1016/j.rser.2016.04.031.
11. Urieli I, and Berchowitz DM. Stirling cycle engine analysis. 1984, Accessed 18 Mar 2022.
12. Abbas M, Said N, Boumeddane B. Thermal analysis of Stirling engine solar driven. Rev Energ Renouvelables. 2008; 11
13. Babaelahi M, Sayyaadi H. Simple-II: a new numerical thermal model for predicting thermal performance of Stirling engines. Energy. 2014;69:873–90. https://doi.org/10.1016/j.energy.2014.03.084.
14. Babaelahi M, Sayyaadi H. A new thermal model based on polytropic numerical simulation of Stirling engines. Appl Energy. 2015;141:143–59. https://doi.org/10.1016/j.apenergy.2014.12.033.
15. Babaelahi M, Sayyaadi H. Analytical closed-form model for predicting the power and efficiency of Stirling engines based on a comprehensive numerical model and the genetic programming. Energy. 2016;98:324–39. https://doi.org/10.1016/j.energy.2016.01.031.
16. Babaelahi M, and Sayyaadi H. Modified PSVL: a second order model for thermal simulation of Stirling engines based on convective-polytropic heat transfer of working spaces, Appl Therm Eng.2015; 85. doi: https://doi.org/10.1016/j.applthermaleng.2015.03.018.
17. Cheng C-H, Phung D-T. Numerical and experimental study of a compact 100-W-class β-type Stirling engine. Int J Energy Res. 2021;45(5):6784–99. https://doi.org/10.1002/er.6271.
18. Elsonbati A, "Stirling Engine Design Manual Second Edition".
19. Tzouganakis P, Kalligeros C, Papalexis C, Koronaki I, Antonakos G, Spitas V. A new second order thermal model for accurate simulation of the time-dependent and steady–state response of beta-type Stirling engines based on time-varying calculation of thermal losses. Int J Eng Res. 2022;24:2739–60.
20. Creyx M, Delacourt E, Morin C, Desmet B, Peultier P. Energetic optimization of the performances of a hot air engine for micro-CHP systems working with a Joule or an Ericsson cycle. Energy. 2013;49:229–39.
21. Wojewoda J, Kazimierski Z. Numerical model and investigations of the externally heated valve Joule engine. Energy. 2010;35(5):2099–108.
22. Lontsi, F., Castaing-Lavignottes, J., & Stouffs, P. (2008). Dynamic simulation of a small Joule cycle Ericsson engine: first results. In *Proc. of the int. stirling forum 2008*. ECOS GmbH Osnabrück, Germany.
23. Komninos NP, Rogdakis ED. Numerical investigation into the effect of compressor and expander valve timings on the performance of an Ericsson engine equipped with a gas-to-gas heat exchanger. Energy. 2018;163:1077–92.
24. Winroth PM, Ford CL, Alfredsson PH. On discharge from poppet valves: effects of pressure and system dynamics. Exp Fluids. 2018;59:1–15.
25. Soyhan H, Yasar H, Walmsley H, Head B, Kalghatgi G, Sorusbay C. Evaluation of heat transfer correlations for HCCI engine modeling. Appl Therm Eng. 2009;29:541–9. https://doi.org/10.1016/j.applthermaleng.2008.03.014.